AN ADAPTIVE APPROACH TO DUCT OPTIMIZATION OF AN INDUSTRIAL BOILER AIR SUPPLY SYSTEM USING AIRFOILS

by

Branimir B. STOJILJKOVIĆ[a*] ***and Marta R. TRNINIĆ***[b]

[a] Faculty of Transport and Traffic Engineering, University of Belgrade, Belgrade, Serbia
[b] Department – Belgrade Polytechnic, Academy of Technical Applied Studies Belgrade, Belgrade, Serbia

Original scientific paper
https://doi.org/10.2298/TSCI210206157S

The purpose of this paper is to examine the pressure drop caused by placing an airfoil at different angles of attack in the straight part of the rectangular air duct, as the first step of investigating the possibility of using a staggered cascade of airfoils for gradual deflection of the air-flow in radial elbows of an air supply system used in industrial boilers. The initial problem was approached by using the commercial CFD code based on the finite volume method to numerically simulate a 2-D incompressible turbulent flow and by conducting direct experimental measurements in the wind tunnel. The results of CFD simulations have been compared to experimentally measured data for two considered cases of inlet velocities and five different angles of attack. Numerical solutions show an adequate level of agreement with experimental measurements. The obtained results indicate the possibility of using a staggered cascade of airfoils for gradual deflection of the air-flow.

Key words*: air duct, air-flow, airfoil, wind tunnel, CFD, pressure drop*

Introduction

The occurrence of turbulence, noise and vibrations in air ducts (channels) are the most often considered problems in the field of ventilation and air conditioning [1-3]. The research results indicate that vibrations can occur due to inefficient construction of the air ducts. Moreover, the analyses of air ducts indicate that the application of turning vanes and radiuses at elbows alleviates the occurrence of turbulent flow, fig. 1.

Figures 1(b) and 1(a) show a flow pattern occurring in a 90° rectangular elbow with and without a turning vane. Figure 1(c) shows a flow pattern that occurs in an elbow with a moderate radius. The analysis of the fluid-flow in the air ducts of industrial boilers in order to reduce vibrations and achieve a smaller pressure drop at the outlet requires the integration of numerical and experimental approaches. The results of the analysis of the existing solutions (a 90° rectangular elbow and a radius elbow), using CFD techniques, are shown in figs. 2 [4] and 3, and can also be found in [5, 6].

Change of flow pattern in air ducts with a radius occurs due to the action of centrifugal force, which makes it significantly different from the flow in air ducts without a radius. The intensity of the centrifugal force depends both on the local axial velocity of fluid particles and the curvature diameter. The action of the centrifugal force, caused by the curvature of the air duct, produces two primary effects on air-flow. First, since air particles near the axis of the air

[*] Corresponding author, e-mail: b.stojiljkovic@sf.bg.ac.rs

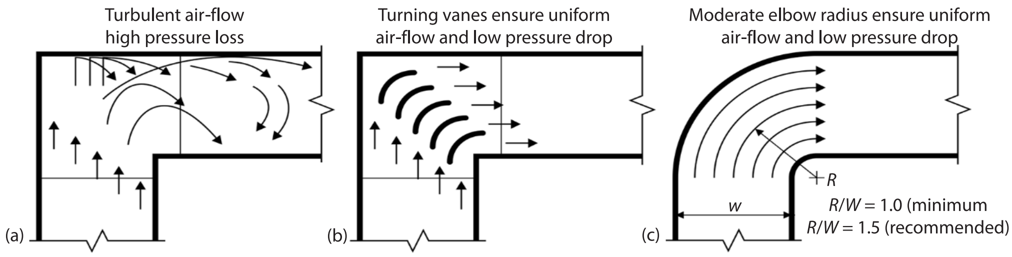

Figure 1. Flow pattern; (a) 90° rectangular elbow, (b) 90° rectangular elbow with turning vanes, and (c) 90° elbow with a moderate radius

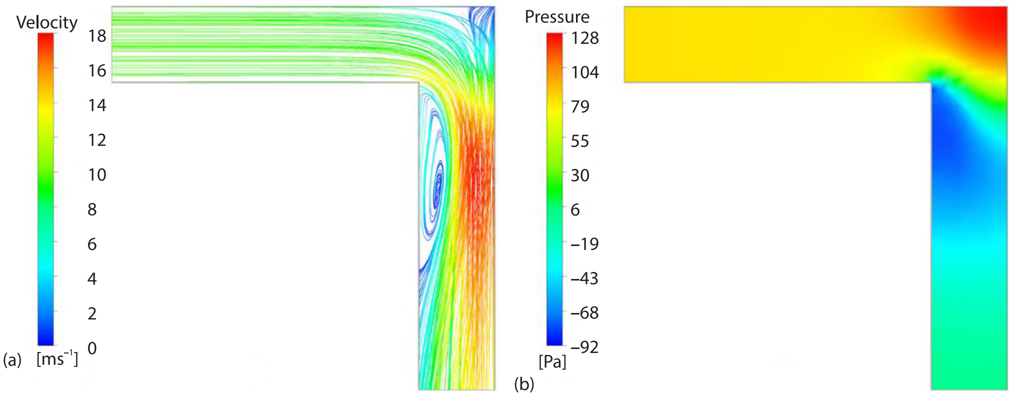

Figure 2. The CFD analysis for a 90° rectangular elbow and inlet velocity of 10 m/s; (a) velocity field and (b) pressure field

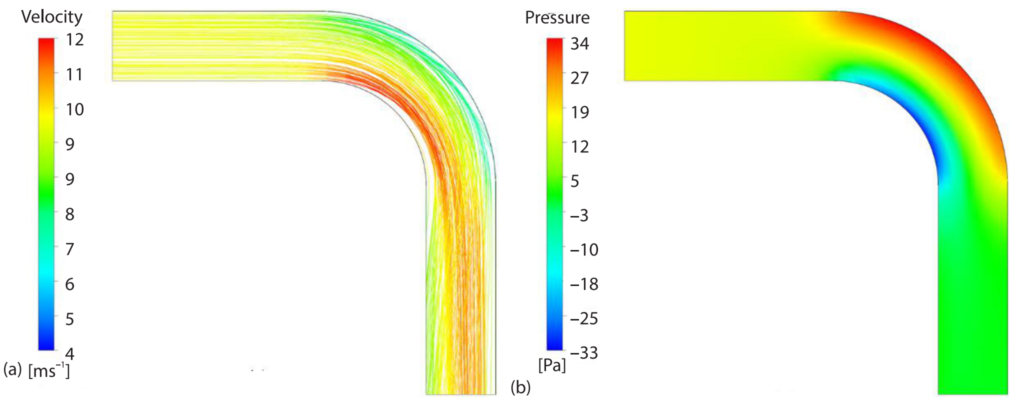

Figure 3. The CFD analysis for a 90° radius elbow and inlet velocity of 10 m/s; (a) velocity field and (b) pressure field

duct have a higher velocity than those near the duct wall, the action of centrifugal force on air particles near the duct wall is less compared to its action on air particles near the duct axis. The air from the central flow area is pushed towards the outer duct wall (the cross-sectional area furthest from the center of the curvature), away from the duct axis. Next, the centrifugal force causes a positive radial pressure gradient, directed from the inner to the outer duct wall, whose intensity is determined by the axial flow velocity. The secondary flow direction is opposite to the action of the radial pressure field and becomes damped by the viscous force. The combined action of the positive radial pressure gradient and the viscous force leads to the formation of a stagnant fluid region near the outer duct wall. By exceeding a critical value of the volume flow, the radial pressure gradient exceeds the value corresponding to the equilibrium conditions in the stagnant region on the outer duct wall and causes a local circulating flow that forms additional vortex pairs. The phenomenon described is known as Dean instability [7]. In an elbow with a moderate radius, the vortex areas are smaller, the velocity profile is better balanced, and the pressure drop is less pronounced.

The basic idea of the adaptive approach is to study the possibility of using a staggered cascade of airfoils, fig. 4, for the gradual deflection of air-flow in the radial elbow of an air duct. The initial step of elaborating this idea was to examine the influence of a single airfoil on the pressure drop in a straight part of an air duct, as a primary aim of this paper. The obtained results could be used as guidelines for further development of the application of a staggered cascade of airfoils.

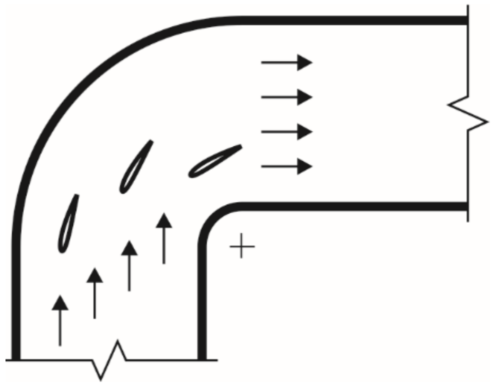

Figure 4. A staggered cascade of airfoils

Description of the adaptive approach

The basic parameters for efficiency analysis and evaluation of boiler plant operation are fuel characteristics, fuel flow, atomization, operating temperature, flue gas emission values [8]. All of these aspects are of great importance. However, they are linked inextricably to one of the main elements of pure combustion, which is often not considered enough: the air needed for combustion. Only a separately dimensioned combustion air supply system can provide a broad control range, stable combustion, and the most suitable flue gas emission values. Accordingly, the adaptive approach should give special attention this seemingly secondary problem, *i.e.* the analysis of the air supply system (lay-out, position, type and number of airfoils in the staggered cascade). Air ducts have been found to have a significant impact on the air-flow quality, pressure drops, and thus on the efficiency of combustion in the boiler. Namely, during the operation of the boiler, the air-flow in the air ducts is turbulent, conditioned not only by the air-flow velocity but also by the shape of the air ducts. Turbulent air-flow, among other things, causes vibrations that interfere with the optimal operation of the boiler.

For more efficient boiler operation, it is necessary to provide laminar flow in air ducts, *i.e.* to reduce the air-flow resistances. Detailed analysis of the air-flow in the existing air duct construction suggests that reducing the resistance to air-flow through the air ducts may be achieved by changing the shape of the air duct construction itself. The authors assume that the proposed adaptive approach (new design of elbows) would provide smaller pressure drops and alleviate the occurrence of turbulence, thus satisfying the basic requirements for stable operation of the boiler.

Problem analysis

Parameters and quantities that characterize the air-flow in the air ducts are essential for the validity of the proposed solution regarding the support of standardized values (air-flow velocities, pressure drops). The solutions eligible for consideration depend on several influencing factors, parameters, and quantities, including the amount of air supplied, air parameters (pressure, velocity), shape, number, and characteristics of the air supply system elements (geometric size of air ducts - length, cross-section). The usual design of air supply systems (our case: air ducts) uses simplified methods to define individual parameters, and air-flow quantities in air ducts (diagrams, tables, formulas) [9, 10].

Modern methods, using CFD techniques, enable obtaining a complete picture of a flow pattern, with a series of details about individual parameters and air-flow quantities. To get more accurate results and optimize the air-flow during the design phase of air supply systems with complex geometry, the use of CFD techniques is necessary today.

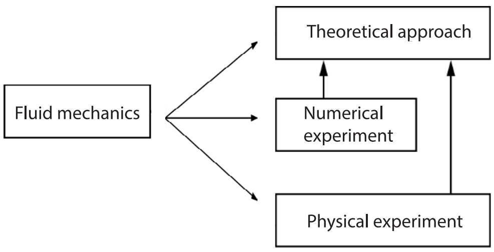

Figure 5. Approaches to solving the problem of fluid mechanics [11]

Since turbulent flow occurs in nature in most cases, which cannot be described analytically due to its chaotic behavior, physical experiments have been resorted to in the past. Today, with the development of computers, conditions have been created for the numerical solution of various mathematical models, which has made it possible to perform experiments numerically. Figure 5 presents the mentioned division of the approach to solving the problem of fluid mechanics. The physical experiments take place in wind tunnels (whether it is a prototype or a physical model).

Experimental tests (using physical models) of complex phenomena are expensive and time-consuming, both in preparation and execution, and require a larger number of repetitions. It is especially necessary to take into account the satisfaction of similarity conditions between the physical model, which often cannot be satisfied, in contrast to the numerical approach, which does not have this problem. The development and validation of numerical models enable numerical experiments to become an increasingly reliable engineering tool, which can always be verified further with available physical experiments. Numerical simulations provide a complete picture of a flow pattern, thus shortening the design time and costs. Unlike physical tests, changing the geometry of the observed object or flow conditions is relatively easily accomplished in numerical experiments. Numerical simulation flow is:

– Defining the problem and the mathematical model:
  - Selection of a mathematical model for the physicality of the observed problem.
  - Setting boundary conditions.
– Numerical solution of a mathematical model:
  - Discretization of the mathematical model equations.
  - Numerical solution of the obtained systems of equations.
– Solution analysis:
  - Numerical and visual interpretation of results.

Numerical model

The picture of a flow pattern, which, by its physical properties is of a spatial and turbulent character, has a crucial role in solving and describing the interaction between air and air ducts. The definition of such a complex flow, resulting from the geometry of the air duct, is based on the basic principles of fluid mechanics contained in the balance equations [12]. Conservative form of the governing equations of incompressible fluid-flow can be written using Cartesian tensor notation:

– time-averaged continuity equation

$$\frac{\partial U_i}{\partial x_i} = 0 \tag{1}$$

– the RANS equations

$$\frac{\partial}{\partial t}\left(\rho U_i\right) + \frac{\partial}{\partial x_j}\left(\rho U_i U_j\right) = -\frac{\partial p}{\partial x_i} + \frac{\partial}{\partial x_j}\left[\mu\left(\frac{\partial U_i}{\partial x_j} + \frac{\partial U_j}{\partial x_i}\right)\right] + \frac{\partial}{\partial x_j}\left(-\rho\overline{u_i' u_j'}\right) \tag{2}$$

– the modelled averaged energy balance equation

$$\frac{\partial}{\partial t}\left(\rho E\right) + \frac{\partial}{\partial x_i}\left[U_i\left(\rho E + p\right)\right] = \frac{\partial}{\partial x_j}\left[\left(\lambda + \frac{c_p \mu_t}{\mathrm{Pr}_t}\right)\frac{\partial T}{\partial x_j} + U_i\left(\mu + \mu_t\right)\left(\frac{\partial U_i}{\partial x_j} + \frac{\partial U_j}{\partial x_i}\right)\right] \tag{3}$$

Reynolds stresses are modelled using Boussinesq's hypothesis, which introduces the notion of turbulent (or eddy) viscosity, μ_t, to relate the Reynolds stresses, τ_{ij}, to the mean strain rate tensor, S_{ij}, therefore, to the mean velocity gradients:

$$\tau_{ij} = -\rho\overline{u_i' u_j'} = 2\mu_t S_{ij} - \frac{2}{3}\rho k \delta_{ij} = \mu_t\left(\frac{\partial U_i}{\partial x_j} + \frac{\partial U_j}{\partial x_i}\right) - \frac{2}{3}\rho k \delta_{ij} \tag{4}$$

Since the air, as a primary fluid, is considered to be a perfect gas, its density can be determined using the equation of state:

$$\rho = \frac{p}{\mathrm{R}T} \tag{5}$$

and the value of specific enthalpy is defined:

$$h = c_p T \tag{6}$$

Closing the system of eqs. (1)-(6) and determining the kinetic energy of turbulence is accomplished using the standard two-equation k-ε turbulence model [13, 14]. The reason for choosing this universal model of turbulent stresses is its proven reliability in flow pattern prediction at Mach numbers significantly less than one. As its name suggests, this model is defined using two additional balance equations:

– transport equation of turbulent kinetic energy, k

$$\frac{\partial\left(\rho k\right)}{\partial t} + \frac{\partial}{\partial x_i}\left(\rho k U_i\right) = \frac{\partial}{\partial x_j}\left[\left(\mu + \frac{\mu_t}{\mathrm{Pr}_k}\right)\frac{\partial k}{\partial x_j}\right] + \tau_{ij}\frac{\partial U_j}{\partial x_i} - \rho\varepsilon \tag{7}$$

– transport equation of the rate of dissipation of turbulent kinetic energy, ε

$$\frac{\partial\left(\rho\varepsilon\right)}{\partial t} + \frac{\partial}{\partial x_i}\left(\rho\varepsilon U_i\right) = \frac{\partial}{\partial x_j}\left[\left(\mu + \frac{\mu_t}{\mathrm{Pr}_\varepsilon}\right)\frac{\partial\varepsilon}{\partial x_j}\right] + C_{1\varepsilon}\tau_{ij}\frac{\partial U_j}{\partial x_i}\frac{\varepsilon}{k} - C_{2\varepsilon}\rho\frac{\varepsilon^2}{k} \tag{8}$$

The turbulent viscosity is modelled:

$$\mu_t = \rho C_\mu \frac{k^2}{\varepsilon} \tag{9}$$

Table 1 lists the values of empirical constants used in this model, together with the turbulent Prandtl number and the turbulent Schmidt number.

Table 1. Empirical constants in the standard *k*-*ε* turbulence model [14]

C_i	$C_{1\varepsilon}$	$C_{2\varepsilon}$	Pr_k	Pr_ε	Pr_t	Sc_t
0.09	1.44	1.92	1.0	1.3	0.85	0.70

Three boundary conditions for the computational domain have been defined [13]:

– Known parameters at the air duct inlet are: U_{in} is the measured inlet velocity, $k_{in} = 1.5(I \cdot U_{in})^2$ is the turbulent kinetic energy, $I = 0.16\ \mathrm{Re}_D^{-1/8}$ is the turbulence intensity, and $\varepsilon_{in} = C_\mu^{3/4} k^{3/2}/(0.07D)$ is the turbulent dissipation rate.
– The no-slip condition is applied at the wall.
– At the air duct outlet, gradients of the flow parameters in the flow direction are equal to zero.

The wind tunnel experiment

The wind tunnel experiment was conducted to analyze the flow pattern around NACA 2412 airfoil at different angles of attack and inlet air velocities and to measure total air pressure at the outlet. First, the experiment was performed in a closed type, subsonic wind tunnel, powered by a frequency-controlled electric fan motor capable of generating air velocities up to 30 m/s in the test section of the wind tunnel, with a rectangular cross-sectional area of 400 mm × 450 mm. A Pitot-static tube was installed at the inlet of the test section measure air velocity, while total pressure was constantly monitored at the outlet using the DSP pressure sensor (Bosch's BMP280). All sensors were connected to the data acquisition unit (DSP pressure sensor to Arduino Mega and Pitot-static tube outputs to PCE PFM 2 micro nanometer). After the calibration procedure, the air velocity was gradually increased and then held at several constant values within the operating range between 5 m/s and 20 m/s to achieve steady flow conditions during inlet velocity and outlet pressure measurement. This procedure was then repeated for different angles of attack. The experimental set-up is presented in fig. 6.

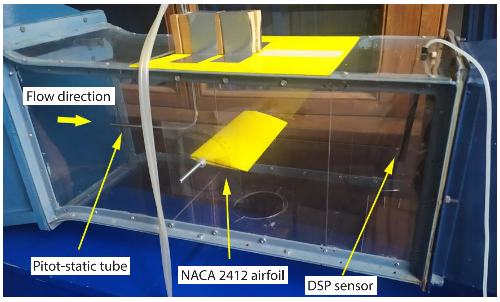

Figure 6. The experimental set-up with sensor positions in the mini wind tunnel

Numerical simulation

The air-flow over the airfoil has been simulated by solving the numerical model equations with a 2-D CFD code using ANSYS Fluent. Numerical simulations were carried out for two inlet velocities (5 m/s and 16 m/s) and five different angles of attack (–10°, –5°, –0°, 5°, and 10°). Figure 7 depicts a computational domain for the angle of attack of –10°.

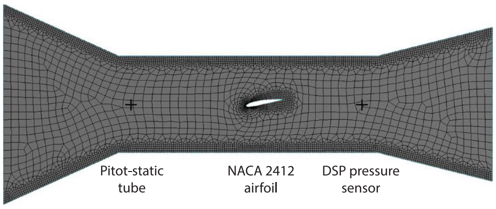

Figure 7. Domain division for CFD simulation (coarse grid)

The computational domain was modelled from the actual geometry of the wind tunnel at the full scale. It includes three basic parts of the wind tunnel: effuser, test section, and diffuser. The unstructured mesh was created for the whole computation domain. Mesh refinement was applied at the regions near the walls and near the airfoil upper and lower surface. To study the effects of the grid on CFD simulation, a comparison with the experimental data, tab. 2, was done for three different sizes of the grid, for which the element size parameter was set relative to the chord length of an airfoil: coarse (20% of the chord length, *i.e.* 0.02 m, which is also the FLUENT Meshing default grid size), medium (10% of the chord length, *i.e.* 0.01 m) and fine (5% of the chord length, *i.e.* 0.005 m).

Table 2. Effects of the grid size for inlet velocity of 16 m/s

AOA [°]	Experiment	Coarse grid		Medium grid		Fine grid	
	Gauge pressure [Pa]	Gauge pressure [Pa]	Discrepancy [%]	Gauge pressure [Pa]	Discrepancy [%]	Gauge pressure [Pa]	Discrepancy [%]
–10	131.66	152.40	16.20	143.29	9.25	135.28	3.15
0	110.27	132.93	20.55	128.03	16.10	109.12	1.05
10	133.87	126.25	5.70	124.44	7.04	129.75	3.08

Based on the obtained results, the fine grid size was chosen for all of the rest CFD simulations. The discrepancy is the smallest, compared with the other cases for each of the tested angle of attack. At the same time, the overall calculation time, including mesh generation, was quite acceptable. In this way, the final mesh was defined with a total cell number of 28546 elements or 29791 nodes. The computation results have shown a very good agreement with the data obtained by the experiment and thus further development of the finer mesh was not necessary. The CFD simulations were performed using 2-D steady-state, pressure-based solver, RANS approach with the k-ε turbulence model. The model constants were set as stated in tab. 1. The boundary condition at the effuser inlet was set as the *inlet velocity* boundary condition type. Velocities were set at the values corresponding to measured velocities at the inlet of the wind tunnel test section, considering the equal volume flow rate through the effuser. At the outlet of the diffuser, the boundary condition was set as the *pressure outlet* boundary with a zero gauge pressure. The values of turbulence quantities at the boundary were specified uniformly. Second-order discretization schemes were used for the convective and diffusion terms of the governing equations. The resulting flow pattern for one of the considered cases is shown in figs. 8 and 9.

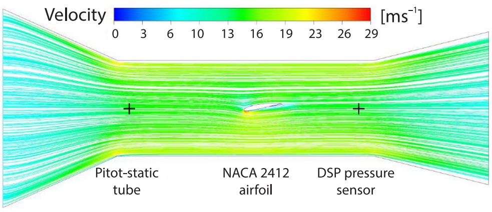

Figure 8. Velocity field for the inlet velocity of 16 m/s and AOA of –10°

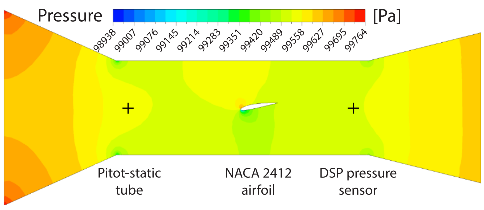

Figure 9. Pressure field for the inlet velocity of 16 m/s and AOA of –10°

As shown in fig. 9, a relatively small pressure drop is observed for the considered case, as well as for all of the analysed cases of different velocities and angles of attack.

Results and discussion

The results of CFD analysis (for inlet velocities 5 m/s and 16 m/s), together with experimentally obtained inlet velocity and outlet pressure data pairs (for all analysed angles of attack within the operating velocity range) and fitted trendlines are presented in fig. 10.

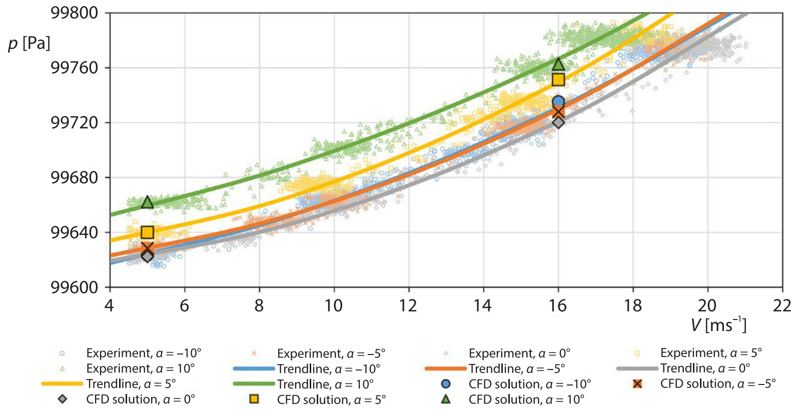

Figure 10. Summary diagram of test results

The experimental data were first filtered to include only data pairs (inlet velocity and total outlet pressure) that were sampled when steady flow conditions were achieved. The method of least squares was then used for fitting a filtered data set with a quadratic function (*i.e.*, $p = a_2V^2 + a_1V + a_0$) for each considered angle of attack separately. The overall second-order polynomial regression model proved to be highly significant since more than 99% of the variance in total pressure at the outlet is predictable from the inlet velocity. Polynomial regression coefficients with corresponding coefficients of determination are given in tab. 3.

Table 3. Regression (trendline equation) coefficients and coefficients of determination

AOA	a_2	a_1	a_0	R^2
–10°	0.3149	3.1588	99600	0.9952
–5°	0.3845	1.2323	99612	0.9974
0°	0.4028	0.4471	99611	0.9980
5°	0.4172	1.3253	99622	0.9959
10°	0.2883	3.7543	99633	0.9942

Summary diagram of test results, fig. 10, confirms that the applied standard *k*-*ε* turbulence model can be used for efficient modelling of air-flow in air ducts with turning vanes in the shape of an airfoil, at an acceptable computational cost.

Table 4. Percent discepancies between experimentally and numerically obtained results

Velocity [ms⁻¹]	Method	Angle of attack [°]				
		–10	–5	0	5	10
		Gauge pressure at the DSP sensor position [Pa]				
5	Experiment	23.667	15.774	12.306	17.057	25.979
	CFD	23.673	16.365	11.329	18.006	29.196
	Discrepancy [%]	0.03	3.74	7.93	5.56	12.38
16	Experiment	131.155	118.149	110.270	128.008	133.874
	CFD	135.282	116.000	109.115	129.382	129.748
	Discrepancy [%]	3.15	1.82	1.05	1.07	3.08

To validate the numerical simulation, a comparison of the gauge pressures at the DSP sensor position, for selected velocities and angles of attack, obtained by experimental tests and numerical simulations, together with percent discrepancies between the two used methods is presented in tab. 4. The maximum difference between experimental and numerical results was less than 8%, except in one of the ten analysed cases when percent discrepancy reached 12.38%, which is still acceptable. Since the results of the comparison indicate that there is a good agreement between the CFD results and experimentally measured data, it can be concluded that the simulated model is well validated.

Conclusions

In this paper, a combined experimental and numerical investigation of the effects of placing a single airfoil at different angles of attack in the straight part of an air duct on the pressure drop was performed. The numerical results were validated by using the experimentally obtained data, indicating that the chosen standard two-equation k-ε turbulence model can be used in further research. The use of an airfoil introduces relatively small pressure losses and opens the possibility of using a staggered cascade of airfoils for gradual deflection of air-flow in radial elbows of an industrial boiler air supply system. Moreover, the research results show that it is possible to actively control the pressure drop at the outlet of an air duct by changing the angle of attack of an airfoil.

The presented results could be used as guidelines for further considerations regarding the lay-out, optimal position and angles of attack, type and number of airfoils in the staggered cascade, as well as analysis of existing turbulent models in order to improve computational efficiency, which will be the subject of further research activities.

Nomenclature

a_0 – regression coefficient, [Pa]
a_1 – regression coefficient, [Pa·sm^{-1}]
a_2 – regression coefficient, [Pa·s^{2}m^{-2}]
$C_{1\varepsilon}$ – empirical constant, [–]
$C_{2\varepsilon}$ – empirical constant, [–]
C_μ – empirical constant, [–]
c_p – specific heat capacity, [Jkg^{-1}K^{-1}]
D – hydraulic diameter, [m]
E – total energy, [Jkg^{-1}]
h – specific enthalpy, [Jkg^{-1}]
I – turbulence intensity, [–]
k – turbulence kinetic energy, [m^{2}s^{-2}]
Pr_k – turbulent Prandtl number for k, [–]
Pr_t – turbulent Prandtl number, [–]
Pr_ε – turbulent Prandtl number for ε, [–]
p – mean static pressure, [Pa]
R – specific gas constant, [Jkg^{-1}K^{-1}]
R^2 – coefficient of determination, [–]
Re_D – Reynolds number (=$\rho UD/\mu$), [–]
Sc_t – turbulent Schmidt number, [–]
S_{ij} – mean strain rate tensor, [s^{-1}]
T – temperature, [K]
t – time, [s]
U_i – mean velocity component, [ms^{-1}]
u_i – fluctuating velocity comp., [ms^{-1}]
V – velocity, [m·s–1]
x_i – position vector component, [m]

Greek symbols

δ_{ij} – Kronecker delta, [–]
ε – dissipation rate of k, [m^{2}s^{-3}]
λ – thermal conductivity, [Wm^{-1}K^{-1}]
μ – molecular viscosity, [Pa·s]
μ_t – turbulent viscosity, [Pa·s]
ρ – density, [kgm^{-3}]
τ_{ij} – Reynolds stress tensor, [kgm^{-1}s^{-2}]

Acronyms

AOA – angle of attack
DSP – digital signal processing

Subscripts

i, j – axis indices (i = 1, 2, 3, j = 1, 2, 3)
in – inlet

References

[1] Mihailović, M., *et al.*, Solution for Eliminating Noise from the Installation of Air Conditioning (in Serbian), *Proceedings*, 27th International Congress on Process Engineering – Processing '14, Belgrade, Serbia, 2017, Vol. 27, pp. 1-19
[2] Bekavac, V., Noise Problems of Air Conditioning Plants (in Serbian), KGH – Heating, *Ventilation and Air-Conditioning*, *45* (2017), 2, pp. 81-92
[3] Ver, L. I., Beranek, L. L., *Noise and Vibration Control Engineering: Principles and Applications*, John Wiley & Sons Inc., Hoboken, N. J., USA, 2006
[4] Trninić, R. M., *et al.*, Air Duct Modificationwards Outlet Pressure Drop and Vibration Level Reduction (in Serbian), *Tehnika*, *75* (2020), 4, pp. 457-466
[5] Kumar, R. S., Pentakota, A. K., Computational Fluid Dynamics Simulations of Pipe Elbow Flow, *International Journal of Professional Engineering Studies*, *9* (2017), 2, pp. 1-10
[6] Didwania, M., *et al.*, Analysis of Turbulent Flow over a 90° Bend of Duct Using in Centralized A. C. Plant by CFD Code, *IOSR Journal of Mechanical and Civil Engineering*, *11* (2014), 4, pp. 41-48
[7] Li, Y., *et al.*, Dean Instability and Secondary Flow Structure in Curved Rectangular Ducts, *International Journal of Heat and Fluid-Flow*, *68* (2017), Dec., pp. 189-202
[8] Bhatia, A., *Improving Energy Efficiency of Boiler Systems: Quick Book*, CreateSpace Independent Publishing Platform, Sout Carolina, Cal., USA, 2015
[9] Haines, R. W., Myers, M. E., T*he HVAC Systems Design Handbook*, McGraw-Hill Education, New York, USA, 2009
[10] Vandagriff, R., *Practical Guide to Industrial Boiler Systems*, CRC Press, Boca Raton, Fla, USA, 2001
[11] Ivan, B., Drag and Pressure Coefficient Calculation for Subcritical Reynolds Number Flow Around a Cylinder (in Croatian), Undergraduate thesis, University of Zagreb, Faculty of Mechanical Engineering and Naval Architecture, Zagreb, 2016
[12] Vidaković, B. M., Banjac, M. J., Improvement of CFD Models of Tunnel Fire Development Based on Experimental Data, *Thermal Science*, *21* (2017), 13, pp. 705-716
[13] Harlow, F. H., Nakayama, P. I., Transport of Turbulence Energy Decay Rate, Report No.: LA-3854, Los Alamos Scientific Laboratory, N. Mex., United States, 1968
[14] Launder, B., Spalding, D., The Numerical Computation of Turbulent Flows, *Computer Methods in Applied Mechanics and Engineering*, *3* (1974), 2, pp. 269-289

Paper submitted: February 6, 2021
Paper revised: April 15, 2021
Paper accepted: April 22, 2021